Effect of synthesis temperature on the structure, morphology and optical properties of PbS nanostructures prepared by chemical bath deposition method

LF Koao[1], **FB Dejene**[1*] **and HC Swart**[2]

[1]Department of Physics, University of the Free State (Qwaqwa Campus), Private Bag X13, Phuthaditjhaba, 9866, South Africa
[2]Department of Physics, University of the Free State, P.O. Box 339, Bloemfontein, 9300, South Africa.

*Corresponding author: Tel: +27 58 718 5307; Fax: +27 58 718 5444; E-mail: dejenebf@ufs.ac.za

Abstract. Lead sulfide (PbS) powders were prepared by chemical bath deposition (CBD) method by varying the synthesis temperatures. The influence of the synthesis temperature on the structure, morphology and optical properties of PbS nanostructures were investigated. The X-ray diffraction (XRD) patterns of the PbS nanostructures correspond to the various planes of a single phase cubic PbS. It was observed that a decrease in the synthesis temperature resulted into additional diffraction peaks due to the presence of impurity phases. It was observed that the estimated average grain sizes from XRD analysis increased slightly with an increase in the synthesis temperature. The crystallinity of the cubic PbS improved significantly with an increase in synthesis temperature. The surface morphology study revealed nanorod structures at low synthesis temperatures but a cubic structure at the high synthesis temperatures. The reflectance spectra showed a partially increase in percentage reflectance and shift of the absorption edge to a higher wavelength with an increase in the synthesis temperature. An additional absorption band in the visible region (647 nm) emerged with an increase in the synthesis temperature. The band gap energy of PbS was found to decrease with an increase in the synthesis temperature. The maximum luminescence intensity was found at a synthesis temperature of 55 ºC.

1. Introduction

In recent years, interest in the development of the semiconductor nanostructured materials has grown rapidly owing to their unique physical and chemical properties [1]. This is due to their potential application in the area of solar cells, optoelectronic devices, photoconductors, sensor and infrared detector devices. Their attractiveness arises from their low synthetic cost, their solution processing ability and the dependence of their optoelectronic properties as a function of size, shape, doping and surface chemistry [2-3]. PbS nanocrystals are attractive for infrared-related applications because the energy of their first excitonic transition can be easily tuned from the visible to the infrared [4]. As its large exciton Bohr radius (18 nm) [5-6], the effects of strong quantum confinement can be achieved even for relatively large structures [7]. The band gap energy of PbS can changed from 0.39 to the values up to 5.2 eV by varying the shape and size from the bulk materials to nanocrystal structures [8].The preparation of PbS has been explored by a number of methods including sonochemical [5], liquid phase synthesis [9], chemical bath deposition [10] and gas phase synthesis [11]. We have selected chemical bath deposition method owing to its many advantages such as low cost, large area production and simplicity in instrumental operation. The aim of this paper is to investigate the effect of synthesis temperature on the structure, morphology and optical properties of PbS nanoparticles prepared by chemical bath deposition method.

2. Experimental

The preparation of PbS powders were carried out using the following procedure: The PbS precursors were prepared by dissolving 0.13 M of lead acetate, 0.18 M of thiourea and 98.8 mL of ammonia in 400 mL of deionised water, separately. During the preparation of the nano-powders, ammonia was used as a complexing agent. The chemical bath solution was prepared as follows: 60 mL of a lead acetate, thiourea and ammonia solutions were mixed. The amount of solutions of lead acetate, thiourea and ammonia was held constant at ratio of 1:1:1. Each mixture was continuously stirred for 10 minutes whilst varying the synthesizing temperature at 55, 65, 70 and 80ºC, respectively. The PbS particles were washed with 60 mL of acetone and ethanol in that order. The precipitates formed were left overnight and then filtered. The obtained particles were dried at ambient conditions for 5 days and ready to be characterized using various characterization technique. The particle size and morphology and the structural and luminescent properties of the as-synthesized phosphors were examined by means of scanning electron microscopy (SEM), X-ray diffraction (XRD), Uv-vis spectroscopy and Photoluminescence (PL).

3. Results and Discussion

3.1 Structural analysis and Composition analysis

Figure 1(a) shows XRD patterns of PbS powders synthesized at various bath temperatures such as 55, 65, 70 and 80 ºC. All XRD patterns show four maximum peaks observed in the diffractogram at around $2\theta = 25.99, 30.11, 43.09$ and 51.03°. All these peaks corresponding to the cubic phase of PbS matched well with the standard JCPDS card no. (05-0592, a= 5.936 Å). The estimated average value of the cell constant a is 5.934 Å which match perfectly with the standard data. No significant changes were observed for lattice parameter with the variations of the synthesis temperature.

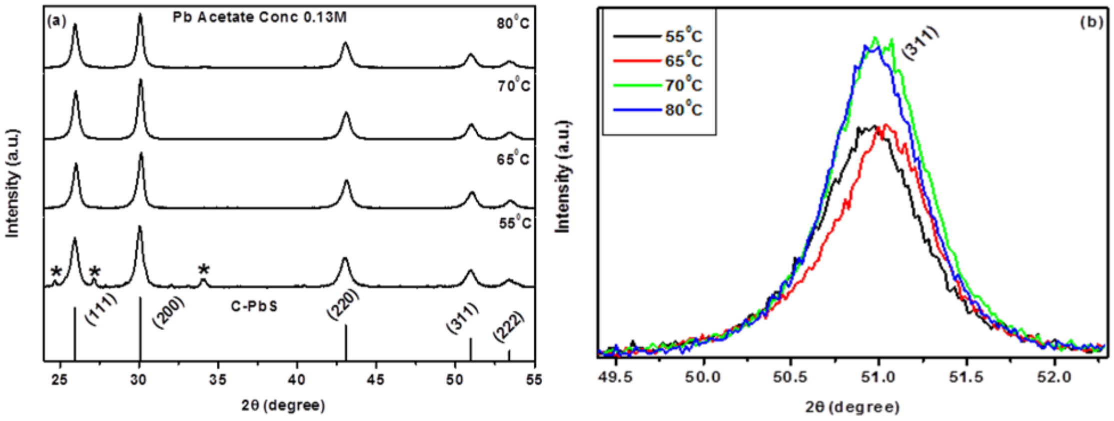

Figure 1. X-ray powder diffraction patterns of PbS (a) prepared at different synthesis temperatures and (b) X-ray powder diffraction patterns of the (111) planes of the PbS powders prepared by the CBD method.

The PbS powder prepared at 55 ºC shows extra peaks which are marked with a star (*) and are due to unreacted lead acetate oxide hydrate due to the low synthesizing temperature. This is confirmed by the JCPDS card no: 18-1740. However, as the bath temperature was increased from 65 to 80 ºC the extra peaks disappear and the intensity of the peaks attributed to PbS improved as shown in Fig. 1(b). This improved intensity with well-defined sharper peaks indicates a high crystallinity of the prepared material. This means that the grain sizes of the PbS powders increases with an increase in the synthesise temperature. The increase in grain size with an increase in synthesis temperature is due to the "Ostwald ripening process" [12]. The average grain size of the as-prepared nanocrystals can be calculated from the Full Width Half Maximum (FWHM) of the diffraction peaks using the Debye-Scherrer formula [13]. All major diffraction peaks for all samples were chosen to estimate the average size of the nano grains by the least square method. From Fig. 2 it is clear that the estimated average particle size increased slightly with an increase in synthesis temperature.

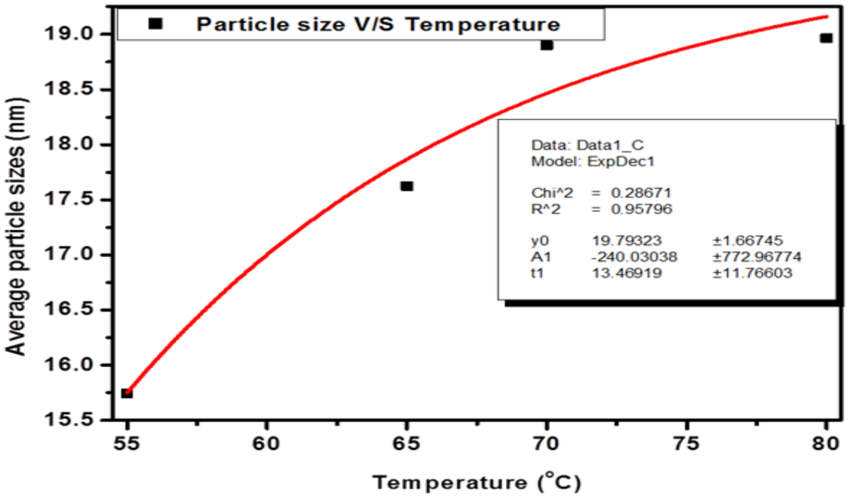

Figure 2. The dependence of average grain sizes of the PbS on the the synthesis temperature of the CBD.

3.2 Surface morphological analysis

Figure 3 (a), (b), (c) and (d) show surface morphologies of the PbS powders synthesized at various temperatures ranging from 55 to 80 ºC. All the samples were taken at 10 keV with a 0.05 nm field of view. The surfaces aspects of the SEM images of the PbS powders are composed of uniform nanorods structures for the synthesis temperature of 55 to 70 ºC, however, the grain size have slightly increased in size with an increase in the synthesis temperature.

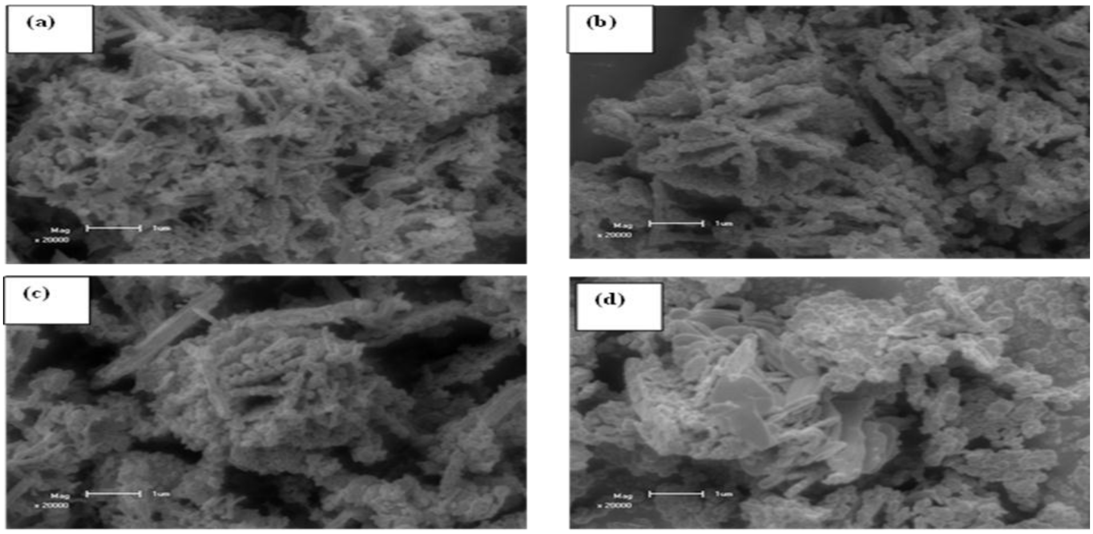

Figure 3: The SEM micrograph of PbS powders synthesized at the various temperatures: (a) 55 ºC, (b) 65 ºC, (c) 70 ºC and (d) 80 ºC.

With further increase in the synthesis temperature to 80 ºC, the nanorods structure broke up in mixed structures with the emergence of spherical nanoparticle and plates-like shapes.

3.3 Optical properties

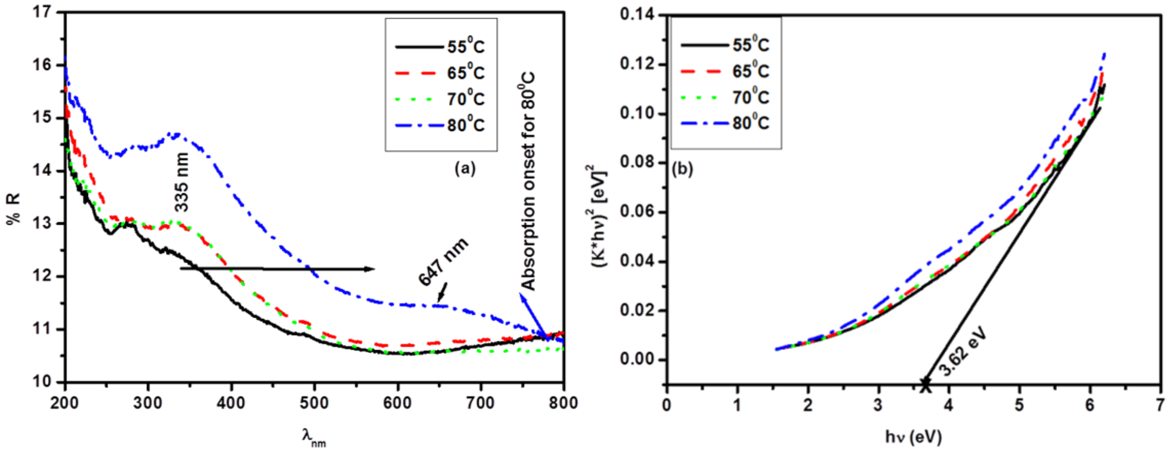

Figure 4. (a) The absorbance spectra and (b) plot to determine the band gap energy of PbS powders prepared at various temperature by the CBD method. The Eg value is marked with a cross.

The UV-visible reflectance spectra of the as prepared samples are illustrated in Figure 4(a). The optical spectra of the samples prepared at 55, 65 and 70 ºC have an absorption onset at about 550 nm, meanwhile in the spectra of the sample prepared at 80 ºC, the onset is observed at about 780 nm. The absorption edge is strongly shifted to higher wavelengths. In addition, the three optical spectra at temperature between 55 and 70 ºC display one well-defined absorption band with a maximum at about 335 nm. At synthesis temperature of 80 ºC an extra absorption band emerges with a maximum at around 647 nm. We can ascribe the origin of the absorption bands at 335 and 647 nm to $1s_e$-$1s_h$ and $1p_e$-$1p_h$ transitions in PbS nanoparticles, respectively [14-15].

Figure 4(b) shows the plot of the band gap energy synthesized at various temperatures estimated using the Kubelka-Munk function remission function [16] for direct transitions. The results reveal that the band gap energy decreased slightly when the synthesis temperature was increased. The value of Eg was determined by plotting tangent line (black solid line) to the curves. The obtained Eg values were found to be 3.63, 3.57, 3.12 and 2.87 eV as synthesis temperature was increased from 55, 65, 70 to 80 ºC, respectively. Their average error analysis is ± 0.35 eV. The decrease in band gap energy and the shift of absorption edges to higher wavelengths can be attributed to the increase in grain size with an increase in synthesis temperature. This result correlates well with the data obtained from the XRD and SEM analysis. The estimated band gap energies are larger than the theoretical band gap (0.39 eV) [17].

3.4 Photoluminescence

Figure 5 depicts the room temperature excitation spectrum of the PbS nanostructures. It can be seen that the excitation spectrum consists of a broad band with a maximum peak at 277 nm whose intensity decreases with the increase in synthesizing temperature. The absorption band may correspond to the $1d_h \rightarrow 1d_e$ transition of PbS **[18-20]**. Figure 6 and 7 shows the PL emission spectra of the PbS nanostructures excited at 277 nm. The emission spectra depict the peaks at around 338, 378 and a less intense broad peak at around 726 nm with a shoulder at around 825 nm. The peaks are associated to the electronic transitions from the $1p_e \rightarrow 1p_h$ (345 nm) and $1s_e \rightarrow 1p_h$ (376 nm) energy levels [18, 21 - 22]. The emissions at 338 nm which arises from the recombination of excitons and/or shallowly trapped electron-hole pairs. The emissions at around 725 and 825 nm are deep level defects. It is clear that the emission bands of the PbS nanostructures did not change, only the emission intensity changed as the synthesis temperature increased. The relative decrease of the PL intensity with the increase in the synthesis temperature, suggested the depletion of the grains which plays a major role in decreasing the defect densities. In other words, their gradual decrease of PL emission intensities reveals a significant decrease in the surface/volume ratio for high temperature grown samples. In this work it was very interesting to find that the grain sizes, morphology, optical and luminescence properties of PbS nanostructures depend on the synthesis temperatures.

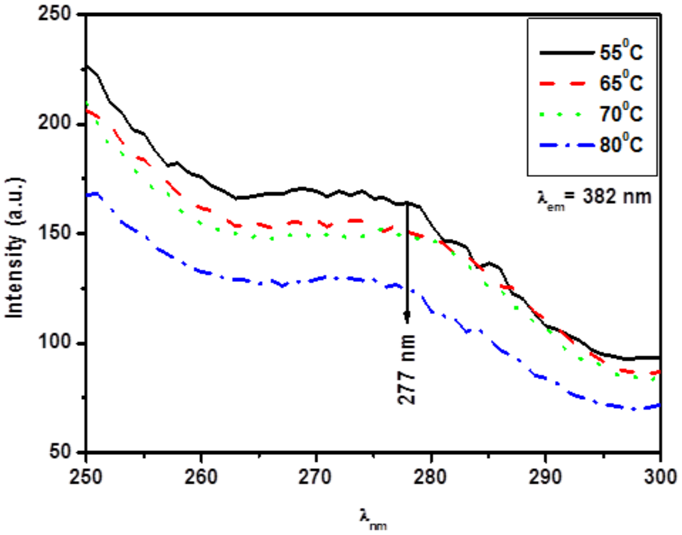

Figure 5. PL excitation spectra of PbS nanostructures prepared at various synthesis temperature emitted at λ_{em} = 382 nm.

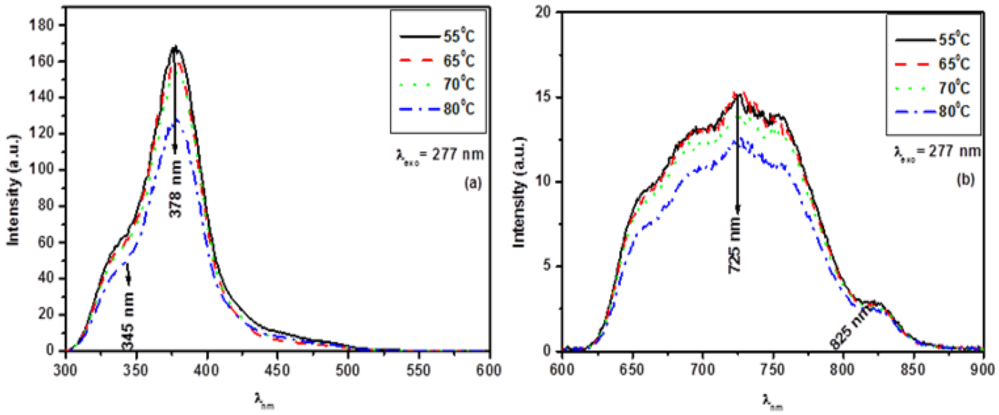

Figure 6. PL emission spectra of PbS nanostructures (a) in visible region and (b) for infrared region synthesized at various synthesis temperatures.

4.1 **Conclusion**

The PbS nanostructures have been successfully synthesized by the chemical bath deposition technique at 55, 65, 70 and 80°C. XRD showed that the structure of the material obtained is cubic PbS. UV spectroscopy showed that the band gap energy of the PbS nanostructures decreased with an increase in the synthesizing temperature. PL showed that the emission intensity of the nanostructures depends on the synthesizing temperatures.

Acknowledgement

The author would like to acknowledge the National Research Foundation, Department of science and technology and the University of the Free State for financial support.

Reference

[1] Xia Y N, Yang P D, Sun Y G, Wu Y Y, Mayers B, Gates B, Yin Y D, Kim F, Yan Y Q, 2003 A*dv. Mater*. **15** 353-389.
[2] Alivisatos A P, 1996 *J. Phys. Chem*. **100** 13226-13239.
[3] Erwin S C, Zu L, Haftel M I, Efros A L, Kennedy T A, Norris D J, 2005 *Nature*. **436** 91-94.
[4] McDonald S A, Konstantatos G, Zhang S, Cyr P W, E. Klem J D, Levina L, Sargent E H, 2005 *Nat. Mater*. **4** 138-142.
[5] Zhou S M, Zhang X H, Meng X M, Fan X, Lee S T, Wu S K, 2005 *J. Solid State Chem*. **178** 399–403.
[6] Zhu J, Liu S, Palchik O, Koltypin Y, Gedanken A, 2000 *J. Solid State Chem*. **153** 342-348.
[7] Dutta A K, Ho T, Zhang L, Stroeve P, 2000 *Chem. Mater.* **12** 1042-1048.
[8] Kumar D, Agarwal G, Tripathi B, Vyas D, Kulshrestha V, 2009 *J. of Alloys and Comp.* **484** 463-466.
[9] Wang C, Zhang W X, Qian X F, Zhang X M, Xie Y, Qian Y T, 1999 *Mater. Lett.* **40** 255-304.
[10] Koao L F, Dejene F B, Swart H C, SAIP’2011 Proceedings, the 56th Annual Conference of the South African Institute of Physics, edited by I. Basson and A.E. Botha (University of South Africa, Pretoria, 2011), p 151-155. ISBN: 978-1-86888-688-3.
[11] Kaito C, Saito Y, Fujita K, 1987 *Jpn. J. Appl. Phys*. **26** 1973-1975.
[12] Krichershy O, Stavan J, 1993 *Phys. Rev. Lett*. **70** 1473-1471.
[13] Cullity B D, 1956 *Elements of X-ray Diffraction (2nd Ed)*, (Addison Wesley) 285-284.
[14] Ai X, Guo L, Zou Y, Li Q, Zhu H, 1999 *Mater. Lett.* **38** 131-135.
[15] Babu K S, Vijayan C, Haridoss P, 2007 *Mater. Sci. Eng C*. **27** 922-927.
[16] RangaRao G, RanjanSahu H, 2001 *Proc. Indian Acad. Sci. (Chem. Sci).* **113** 651-658.
[17] Z. Wang, B. Zhao, F. Zhang, W.Mao, G. Qian, X. Fan, Mater Lett. 61(2007) 3733–3735.
[18] Ai X, Guo L, Zou Y, Li Q, Zhu H, 1999 *Mater. Lett.* **38** 131-135.
[19] Babu K S, Vijayan C, Haridoss P, 2007 *Mater. Sci. Eng C*. **27** 922-927.
[20] Lu S, Sohling U, Krajewski T, Menning M, Schmidt H, 1998 *J. Mater. Sci. Lett.* **17** 2071-2073.
[21] Wang Z S, Yang S, 1999 *Chem.Mater.* **11** 3365-3369.
[22] Li L S, Qu L, Wang L, Lu R, Peng X, Zhao Y, Li T J, 1997 *Langmuir*, **13** 6183-6187.